NASA TN D-3329

# HEAT-SHIELD ABLATION MEASUREMENTS USING RADIOISOTOPE TECHNIQUES

*by George W. Brandon, Jr.*

*Manned Spacecraft Center*

*Houston, Texas*

# HEAT-SHIELD ABLATION MEASUREMENTS

# USING RADIOISOTOPE TECHNIQUES

By George W. Brandon, Jr.

Manned Spacecraft Center
Houston, Texas

## NATIONAL AERONAUTICS AND SPACE ADMINISTRATION

## ABSTRACT

A method is presented for applying nucleonic techniques to the measurement of heat-shield surface recession rates during reentry. The method uses a radioactive "line" source embedded in the heat-shield material. As portions of the radioactive source ablate with the heat-shield during reentry, progressive activity decreases are monitored by a miniaturized detection system. Accuracy of the method is developed and some examples of ablation profiles determined by this method are presented and discussed.

# HEAT-SHIELD ABLATION MEASUREMENTS

## USING RADIOISOTOPE TECHNIQUES

By George W. Brandon, Jr.
Manned Spacecraft Center

## SUMMARY

Detailed, precision measurements of heat-shield surface recession rates during reentry are needed for complete evaluation of heat-shield performance prior to use on manned reentry vehicles. Conventional surface recession-rate measurement systems are incapable of supplying the required accuracy and resolution. A method is described wherein nucleonic techniques are used to provide the needed information. The measurement technique incorporates a radioactive "line" source embedded in the heat-shield. Portions of the source recede with the actual heat-shield surface. Decreases in source activity, continuously monitored by a miniature Geiger-Mueller detection system, can be related to heat-shield thickness. Various sources of potential error are discussed, and estimates of total system accuracy are developed. Finally, some specific data are presented and evaluated.

## INTRODUCTION

The advent of space exploration and manned space travel has created interesting and unique problems concerning methods for protecting an interplanetary vehicle, its crew, and instrumentation against the severely hostile environment encountered during reentry into the earth's atmosphere. In order to insulate a space vehicle and its contents from the extremely high temperatures associated with reentry, current engineering design logic requires that the vehicle be covered with a protective material, or heat-shield, which will absorb and dissipate the heat loads generated during reentry.

While the variety of heat-shield materials now available may be adequate for currently-planned vehicles and missions, ground evaluation of heat-shield performance is, in some cases, handicapped by the lack of suitable test facilities and support instrumentation. Important performance parameters which must be determined during heat-shield material evaluation tests include surface and internal temperatures, incident heating rates, material decomposition (char), and surface erosion (ablation).

Although the ablation process may vary between individual ablator materials, the general characteristics of ablation (ref. 1) remain fairly constant

for most heat-shield materials. During reentry, as the heat-shield surface and internal temperatures increase into the $500^{\circ}$ to $1000^{\circ}$ F range, the material begins to decompose and outgas, or char, removing a portion of the absorbed heat. With further temperature increases, decomposition is completed, leaving only the basic ablator material matrix (carbon, for example), which softens and is finally removed through various combinations of vaporization, dynamic shear, or chemical reaction with the air stream. Ablative materials which follow the same general reaction pattern of first, decomposition (charring); and finally, surface erosion (ablation), are commonly known as "charring ablators".

A number of methods for the measurement of heat-shield surface ablation have been developed, including the use of electrical breakwire gages and mechanical switching devices embedded in the heat-shield. Thus far, however, current methods have not provided the detail required for a complete evaluation of heat-shield performance during reentry.

In an effort to provide reentry measurements which include the small-scale fluctuations of ablation surface recession, a unique system which incorporates nuclear measurement techniques was developed by the National Aeronautics and Space Administration. This nuclear technique has the added advantage of requiring no electrical or mechanical opening or access port through the rear side of the heat-shield structure.

This paper describes the nuclear technique and presents some typical ablation measurements determined by this method. Physical characteristics of the system are described, together with an analysis of the potential accuracies.

## MEASUREMENT TECHNIQUE

### General Description

The general configuration of the complete measurement system is shown schematically in figure 1. The nuclear ablation sensor consists of two interrelated subsystems: (1) a radioactive "line" source embedded in the heat-shield and (2) a detector-signal-conditioning package. Radiations from the source are detected by a miniature Geiger-Mueller detector array located within a few inches of the source. Detector pulses are shaped, amplified, and converted to a dc voltage by an RC integrating circuit.

When portions of the radioactive source ablate at the same rate as the actual heat-shield surface, the total activity detected by the Geiger-Mueller tubes decreases accordingly. The output voltage of the system at any time is, then, proportional to the thickness of the remaining heat-shield at that time or, alternately, to the amount of ablation surface recession. System design and operation are discussed in detail in the following sections.

2

NASA-S-65-5695

Figure 1. - Schematic representation of nuclear heat-shield ablation sensor

## Radioactive "Line" Source

Several criteria must be imposed during the selection of a radioactive source to be used for reentry ablation measurements. The radioactive source must have the following characteristics:
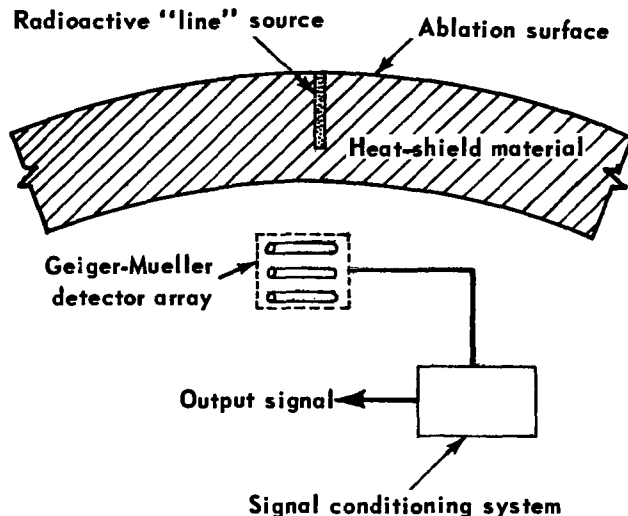
(1) It must maintain structural integrity until exposed to the reentry environment at the ablation surface.

(2) It must not degrade heat-shield performance or introduce any localized ablation discontinuities.

(3) It must contain relatively high-energy gamma-emitting radioisotopes to minimize radiation attenuation through the heat-shield material and substructures.

(4) It must contain the minimum amount of activity commensurate with measurement accuracy requirements. This stipulation is important for the radiological protection of personnel and to minimize specialized handling requirements.

Extensive screening and qualification tests indicate that the optimum source materials and configuration, at least for the charring ablator being considered for use on the Apollo vehicle, consist of a relatively energetic gamma emitter distributed homogenously in a high-temperature silicone carrier material and encased in a small-diameter aluminum oxide tube. A series of arc-jet tests determined that the silicone carrier material possesses thermal properties sufficiently similar to those of the Apollo heat-shield material to insure that the silicone carrier will ablate at the same rate as the surrounding heat-shield surface, at least within the range of reentry conditions anticipated for the Apollo vehicle. The aluminum oxide tube is intended primarily to strengthen the source-carrier material mixture during preparation and installation.

The actual mechanics of the radioactive source performance are relatively simple. As the heat-shield ablation surface recedes during reentry, the extreme upper end of the radioactive source is exposed to the reentry environment.

3

The exposed segment of the aluminum oxide tube and silicone carrier immediately melts and decomposes, releasing a portion of the radionuclide, which vaporizes and is carried overboard.

One important consideration concerns the relative vaporization temperatures of the radionuclide and the silicone carrier material. Low radionuclide melting and vaporization temperatures are of little importance, since the radionuclide is trapped (whether in a liquid or gaseous state) in the silicone carrier until the carrier melts and is removed. It is, however, mandatory that the vaporization temperature of the radionuclide not exceed that of the carrier material, since this condition could result in solid radionuclide material momentarily being deposited on the ablation surface, causing erroneous measurements.

A number of suitable radionuclides with sufficiently long half-lives are available for incorporation into the source materials. Representative radionuclides include (ref. 2) cobalt 60, with gamma energies of 1.17 and 1.33 MeV, and silver 110m, with a maximum energy of 1.52 MeV. For applications during ground tests, a short half-life radionuclide such as gold 198 might be considered to minimize contamination of testing facilities.

It should be emphasized that the source materials and configuration described here are verified for only the current Apollo heat-shield material and would not necessarily be compatible with any other ablator. It is, however, reasonable to assume that careful evaluation of the physical properties of various materials and a detailed analysis of the performance characteristics of any ablator should result in a source configuration applicable to that particular ablator material.

Electronic System

The electronic system (fig. 2) used with the nuclear ablation sensing technique incorporates three Geiger-Mueller detector tubes operating in parallel. Detector pulses are shaped and amplified by transistorized circuitry and introduced into a solid state RC integrating circuit, resulting in a dc output voltage proportional to the frequency of the incoming detector pulses. A dc-to-dc converter supplies the 600 volts required for proper operation of the Geiger-Mueller Tubes.

Component values of the integrating circuitry are selected to provide a 5 V dc output signal at a maximum input pulse rate of 3000 pulses per second. The linearity of the system response does not deviate more than 0.5 percent over the range from 300 to 3000 pulses per second. The pulse integrating portion of the circuitry has a time constant, or RC value, of approximately 0.5 seconds, providing both reasonable accuracy and adequate response. Output signal characteristics are such that the signal may be transmitted, commutated and transmitted, or recorded for delayed transmission or readout.
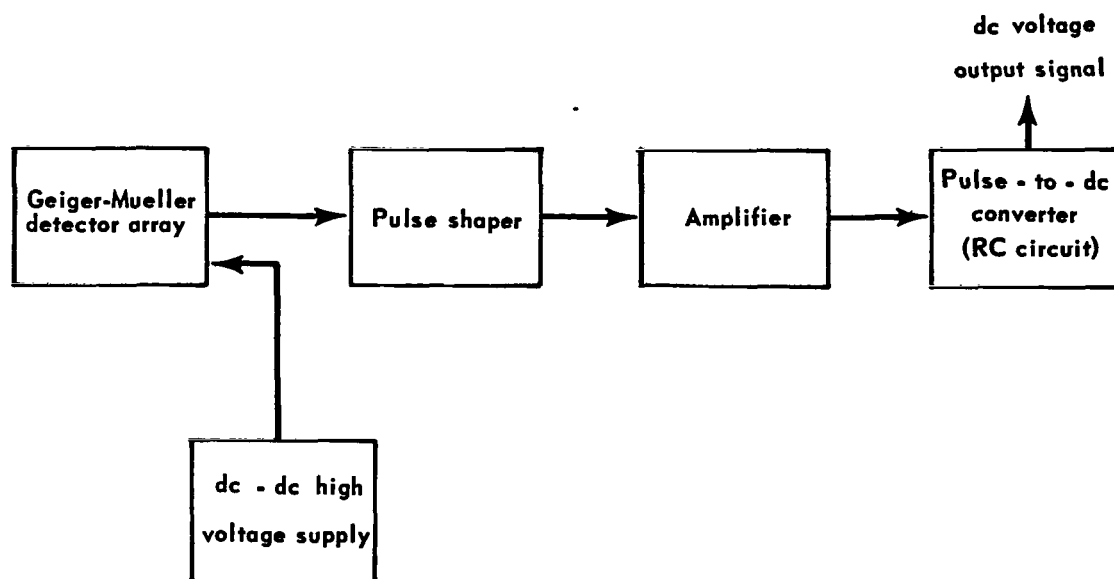
dc voltage

output signal

| Geiger-Mueller detector array | → | Pulse shaper | → | Amplifier | → | Pulse - to - dc converter (RC circuit) |

dc - dc high voltage supply

**Figure 2. - Block diagram of nuclear ablation sensor electronic system**

MEASUREMENT ACCURACY

In order to obtain the maximum accuracy from any measurement system, particularly from a nuclear count rate system, all pertinent sources of error must be completely defined and evaluated.

Error sources applicable to the method under discussion are of two basic types:  first, systematic errors which are caused by basic system limitations and cannot be fully corrected, and second, random errors which may fluctuate as a result of environmental changes or methods of applying the measurement technique.

Systematic Errors

Two sources of error in this particular measurement technique can be classed as systematic.  One error related to any nuclear count rate system is caused by both the statistical fluctuations in the decay of any radioisotope

and the fluctuations inherent to any RC integrating circuit. The other systematic error which cannot easily be eliminated results from variations in the difference between the location of the upper end of the radioactive "line" source and the position of the actual ablation surface.

In an effort to determine the potential magnitude of the errors introduced by the failure of the radioactive source to ablate exactly with the ablation surface, a number of inert models were tested in an arc-jet facility under various representative heating rates ranging from 50 to 550 $Btu/ft^2/sec$. The inert source substitutes were identical to the radioactive sources in all details, except that inert isotopes replaced the radionuclides. Inert isotopes of a given element are identical to radioisotopes of the same element in all chemical and physical properties (refs. 3, 4 and 5), thereby validating the replacement of the radionuclides with inert isotopes.

Results of the inert model tests in arc-jet facilities, summarized in table I, verify that the rms source position error $\sigma_p$ is less than 0.01 inch over the range of heating rates used during the tests.

TABLE I - SUMMARY OF INERT SOURCE SUBSTITUTE EVALUATION TESTS

Number of tests ........................ 43

Maximum position error, in. ............. 0.02

Average position error, in. ............. 0.01

rms position error, $\sigma_p$, in. ........... 0.01

Analysis of the errors associated with any nuclear counting system incorporating an RC integrating circuit (refs. 6 and 7) shows that the rms counting error $\sigma_c$, in counts per second, is directly proportional to the square root of the count rate n and inversely proportional to the square root of twice the time constant RC of the integrating circuit. Expressed mathematically, the rms counting error is then

$$\sigma_c = \sqrt{\frac{n}{2RC}}$$

in counts per second or, as a percentage rms counting error

$$\sigma_{cp} = \frac{\sigma_c}{n} \times 100$$

Values of $\sigma_c$ and $\sigma_{cp}$ for some appropriate values of n are shown in table II.

TABLE II - COMPUTED RMS ERRORS $\sigma_c$ AND $\sigma_{cp}$ AS A FUNCTION OF

COUNTING RATE, n, FOR RC = 0.5 SECOND

| n, counts/sec | $\sigma_c$, counts/sec | $\sigma_{cp}$, percent |
|---|---|---|
| 3000 | 55 | 1.8 |
| 2000 | 45 | 2.2 |
| 1000 | 32 | 3.2 |
| 300 | 17 | 5.8 |

The first value in table II, $\sigma_{cp}$ = 1.8, is the rms error associated with a full-scale input of 3000 pulses per second and represents the maximum accuracy to be expected from the counting system. The next two values, $\sigma_{cp}$ = 2.2 and $\sigma_{cp}$ = 3.2, are values associated with actual mid-range counting rates encountered during typical applications. The last value $\sigma_{cp}$ = 5.8 is considered a worst-case value, since applications are planned to preclude any counting rates of less than 10 percent of the original or full-scale value.

To determine a total rms error $\sigma_T$ for the complete ablation sensor system, it is necessary to combine the two independent rms errors $\sigma_p$ and $\sigma_c$. Representative values of $\sigma_T$ are given in table III for various values of "line" source length L and count rate n. It can be seen from table III that the rms error $\sigma_T$ decreases as the counting rate increases. Similarly for a given value of n, $\sigma_T$ increases as L increases.

TABLE III - ABLATION GAGE TOTAL RMS ERROR, $\sigma_T$, AS A FUNCTION OF L AND n

| Counting rate, pulses/sec | $\sigma_T$, in., for L, in. | | | |
|---|---|---|---|---|
| | 0.5 | 1.0 | 1.5 | 2.0 |
| 3000 | 0.013 | 0.021 | 0.029 | 0.037 |
| 2000 | 0.015 | 0.024 | 0.035 | 0.045 |
| 1000 | 0.019 | 0.034 | 0.049 | 0.065 |
| 300 | 0.031 | 0.059 | 0.088 | 0.116 |

Since typical anticipated ablation depths for the Apollo heat-shield range from 0.5 to 1.5 inches, the errors presented in table III are not excessive for the amount of ablation expected.

### Random Errors

Any nuclear counting system application must give careful consideration to the presence and effects of ambient background radiation levels if maximum reliability is to be placed on the data obtained from the system. During ground or laboratory tests using the nuclear ablation sensor, background radiation levels would normally be essentially non-existent and could be dismissed as possible error sources. In any case, however, background levels should remain relatively constant over short time spans and could be adequately compensated by simple calibration procedures. These procedures might include, as an example, a determination of the magnitude of the system output voltage resulting from the effects of background radiation and the subsequent post-measurement subtraction of this constant background voltage from the actual test data.

Background corrections for flight applications of the nuclear ablation gage are more complex and require a more careful degree of consideration. Although many measurements with comparable Geiger-Mueller detector circuitry during orbital Mercury missions have indicated only minimal radiation levels in reentry corridors at altitudes below the Van Allen belts (refs. 8 and 9), the possibility still exists that intensified solar or cosmic activity could result in elevated background activity at reentry altitudes. Although no generalizations can be made concerning a universal correction technique, it seems entirely logical to assume that adequate corrections could, in most cases, be provided. Applicable procedures might include one of several

relatively simple in-flight calibration techniques or, in more extreme cases, the use of independent detection systems, physically shielded from the radio-active ablation sensor source, for the evaluation of background activity.

Basic calibration requirements are also relatively complex for a continuous-measuring system as opposed to a step-measurement type of sensor. Although it is possible to analytically establish a calibration for the ablation gage, the complex geometries and the necessity for accurately establishing attenuation coefficients and build-up factors preclude useful and routine applications of the analytical approach. Hence, a simplified experimental calibration technique is to be desired.

In practice, this experimental calibration approach requires that the initial activity and length of the flight source be established, either on the actual flight vehicle or by the use of a structurally-identical mockup. A series of calibration sources is then prepared with each source being a different fraction in length of the actual flight source and containing that same fraction of the initial flight source activity. Each calibration source is fitted in turn into the position of the flight source. The resulting system output voltage for each calibration source is then recorded as a function of calibration source length. A typical calibration curve is shown in figure 3.

**NASA-S-65-5691**

| Source | Length, in. | Activity, mci | System output, V |
|--------|-------------|---------------|------------------|
| Flight | 1.0 | 5.0 | 5.0 |
| Calibration 1 | 1.0 | 5.0 | 5.0 |
| Calibration 2 | 0.8 | 4.0 | 4.6 |
| Calibration 3 | 0.6 | 3.0 | 3.9 |
| Calibration 4 | 0.4 | 2.0 | 3.0 |
| Calibration 5 | 0.2 | 1.0 | 1.8 |

O  Experimental calibration

— — —  Theoretical calibration for perfect geometry
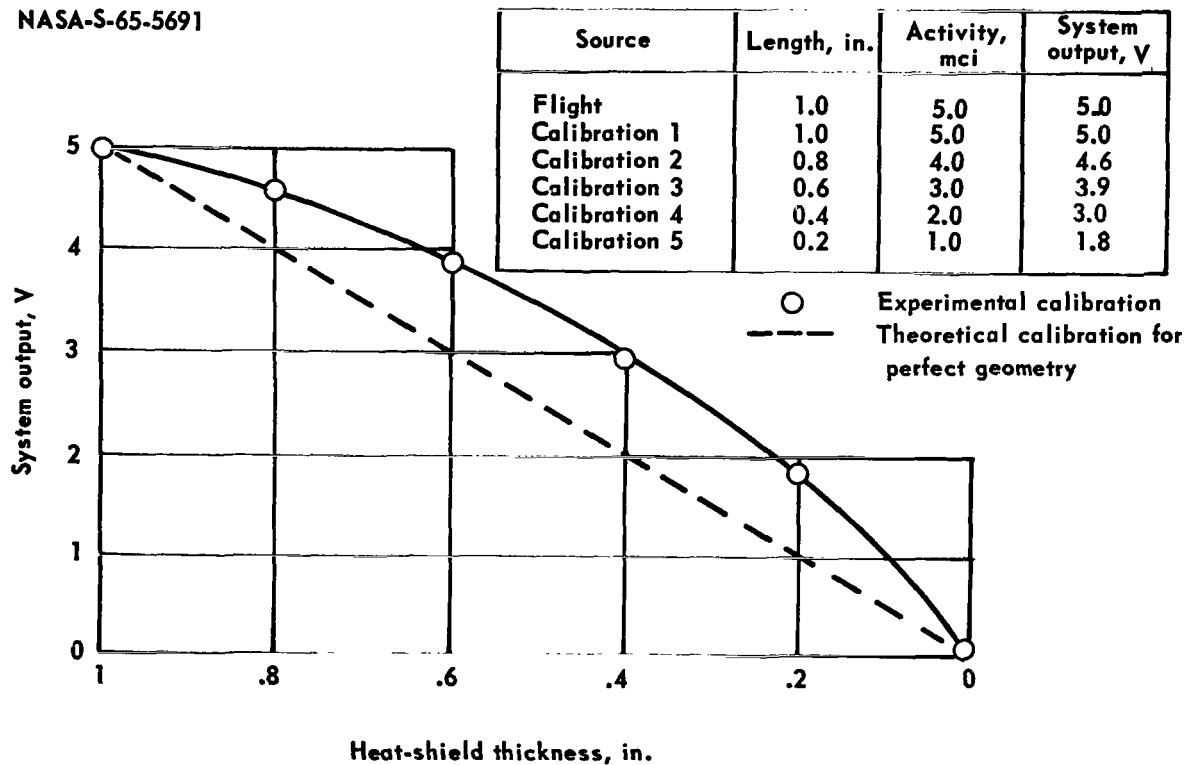


Heat-shield thickness, in.

Figure 3. - Calibration curve for typical nuclear ablation sensor installation

9

In this particular case, the slight convexity of the calibration curve is determined by the source-detector geometry of the particular measurement application.

Other potential sources of error include source linearity, which can be eliminated by careful source preparation, and the effects of data distortion resulting from commutation, recording, or telemetry. Degrees of data distortion vary radically between applications and must be considered separately for each individual application.

EXAMPLES OF MEASUREMENT DATA
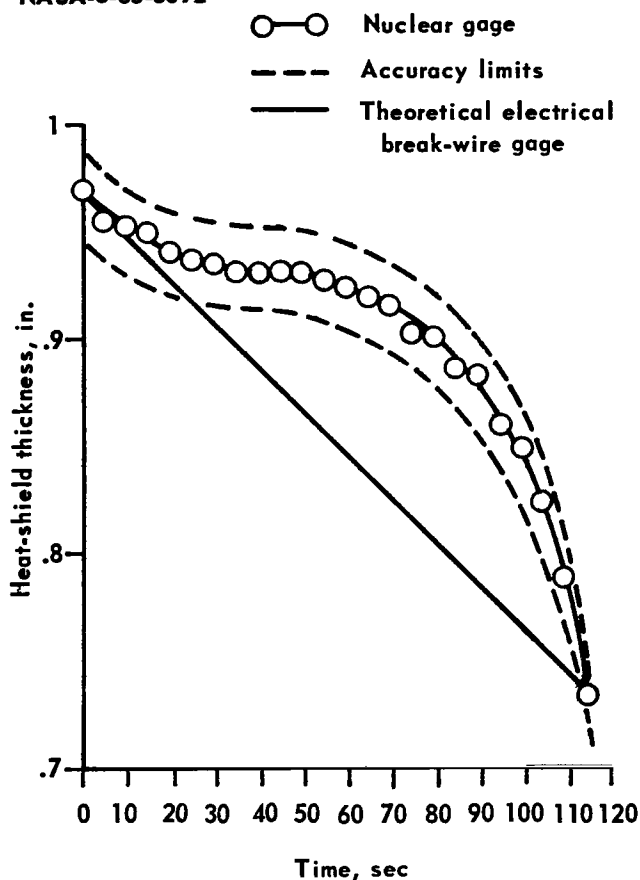
Figure 4. - Comparison of nuclear gage and theoretical electrical break-wire gage ablation profiles

Figures 4 to 6 illustrate three typical sets of data obtained while using the nuclear ablation sensor technique for the ground evaluation of a specific ablator material in an oxygen-acetylene torch facility. Although the amount of detail shown in each figure is, for most applications, sufficient for an adequate determination of ablation rate, even more detail can be obtained by varying the electronic system RC value or counting rate ranges. In each figure, the dotted lines denote the approximate error limits as determined from the values in table III.

Figure 4 represents a test case in which the oxygen and acetylene gas pressures were increased by approximately 75 percent (35 psi to 60 psi) midway in the test, resulting in an increase in ablation rate, probably because of the increased shear forces. In this figure, the straight line represents a typical ablation trace that would have resulted from the use of an electrical breakwire gage with active elements at the original test model surface and at the depth (0.730 inches) reached by the ablation front at the completion of the test. Although nuclear gage and breakwire data would have provided the same initial and endpoint thickness values (within the accuracy limits of the nuclear system), the breakwire
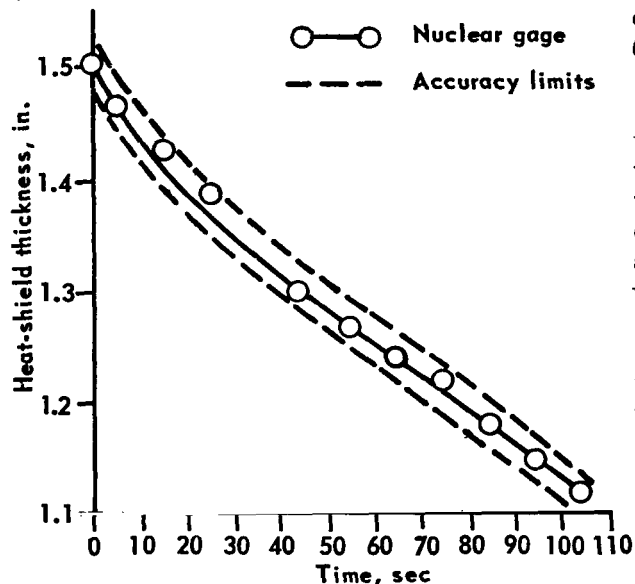
10

Figure 5. - Typical nuclear gage ablation profile

data would not have indicated the increase in ablation rate at approximately 60 seconds after test initiation.

Figures 5 and 6 illustrate other typical ablation traces obtained from the nuclear gage. Although the ablation rates are relatively smooth, several minor ablation rate discontinuities are present. These discontinuities, which would not be evident from an examination of electrical breakwire data, can be resolved only because of the continuous measurement capability of the nuclear gage.
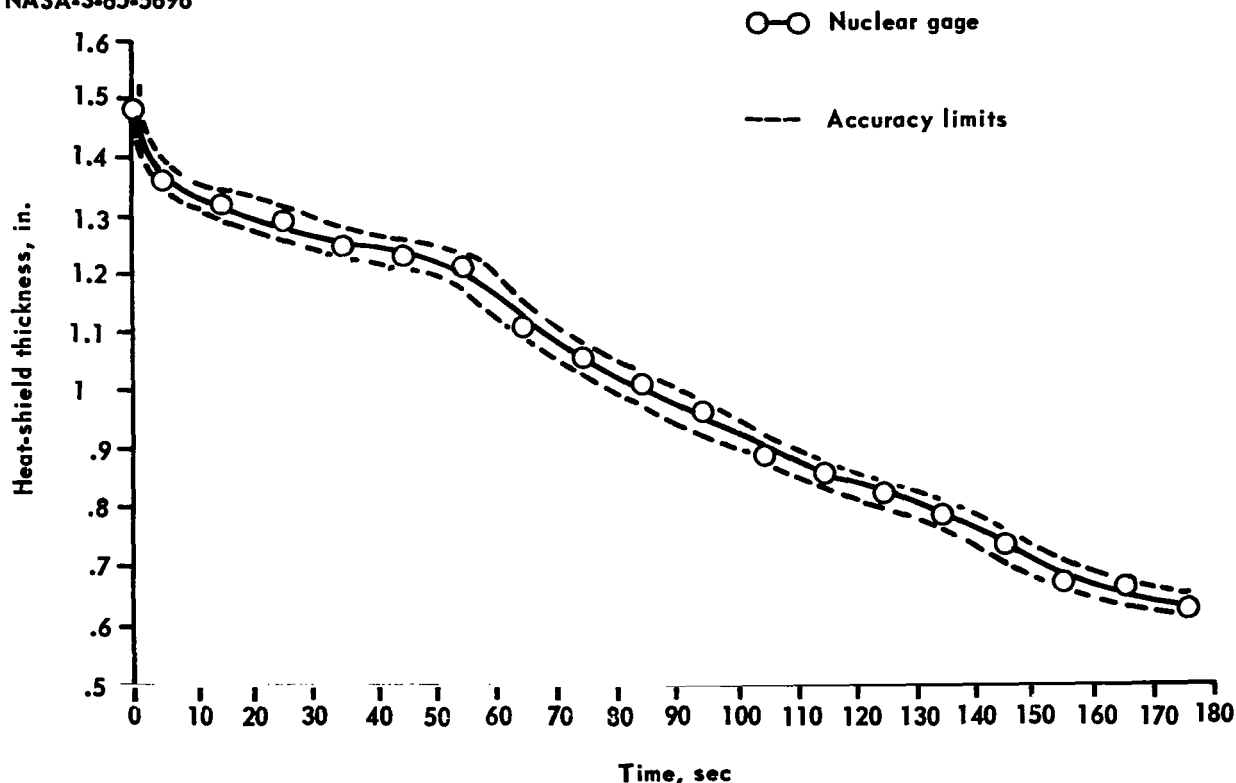


Figure 6. - Typical nuclear gage ablation profile

11

## CONCLUDING REMARKS

A method has been presented for the continuous measurement of heat-shield surface position and surface recession rates during reentry. Such data are necessary for complete evaluation of heat-shield performance prior to applications on manned reentry vehicles. No other method is known which can provide a continuous heat-shield thickness measurement during reentry. Examples of data obtained by this method reveal small-scale ablation rate discontinuities which could not be resolved by previously available ablation sensing systems.

# REFERENCES

1. Davis, W. G.: Heat-Shield Char Determinations Through Nucleonic Techniques, NASA TND - 3264, 1965

2. Anon.: Radiological Health Handbook. OTS Report PB121748R, U. S. Department of Health, Education and Welfare, Public Health Service, Sept. 1960

3. Price, William J.: Nuclear Radiation Detection. McGraw-Hill Book Co., Inc., 1958

4. Evans, Robley D.: The Atomic Nucleus. McGraw-Hill Book Co., Inc., 1955

5. Lapp, Ralph E. and Andrews, Howard L.: Nuclear Radiation Physics. Prentice-Hall, Inc., 1954

6. Richardson, C. H.: An Introduction to Statistical Analysis. Harcourt, Brace and Co., New York 1944

7. Tittle, C. W.: How To Apply Statistics To Nuclear Measurements. Tech. Bulletin 14, Nuclear-Chicago Corp., 1964

8. Warren, Carlos and Baker, Benny R.: Radiation Measurements on the 9th Mercury-Atlas Mission MA-9. NASA TND - 2608, 1965

9. Anon.: The Space Radiation and Its Interactions With Matter. REIC Rep. 37, Radiation Effects Information Center, Battelle Memorial Institute, Jan. 1965

# NASA SCIENTIFIC AND TECHNICAL PUBLICATIONS

**TECHNICAL REPORTS:** Scientific and technical information considered important, complete, and a lasting contribution to existing knowledge.

**TECHNICAL NOTES:** Information less broad in scope but nevertheless of importance as a contribution to existing knowledge.

**TECHNICAL MEMORANDUMS:** Information receiving limited distribution because of preliminary data, security classification, or other reasons.

**CONTRACTOR REPORTS:** Technical information generated in connection with a NASA contract or grant and released under NASA auspices.

**TECHNICAL TRANSLATIONS:** Information published in a foreign language considered to merit NASA distribution in English.

**TECHNICAL REPRINTS:** Information derived from NASA activities and initially published in the form of journal articles.

**SPECIAL PUBLICATIONS:** Information derived from or of value to NASA activities but not necessarily reporting the results of individual NASA-programmed scientific efforts. Publications include conference proceedings, monographs, data compilations, handbooks, sourcebooks, and special bibliographies.

*Details on the availability of these publications may be obtained from:*

SCIENTIFIC AND TECHNICAL INFORMATION DIVISION

# NATIONAL AERONAUTICS AND SPACE ADMINISTRATION

Washington, D.C. 20546